



**Precisely Controlled Molecular Imprinting of Glutathione-s-Transferase by Orientated Template Immobilization Using Specific Interaction with an Anchored Ligand on a Gold Substrate**

Journal:	<i>Polymer Chemistry</i>
Manuscript ID:	PY-ART-03-2014-000350.R1
Article Type:	Paper
Date Submitted by the Author:	07-Apr-2014
Complete List of Authors:	Kamon, Yuri; Kobe University, Graduate School of Engineering Matsuura, Ryo; Kobe University, Graduate School of Engineering Kitayama, Yukiya; Kobe University, Graduate School of Engineering Ooya, Tooru; Kobe University, Graduate School of Engineering Takeuchi, Toshifumi; Kobe University, Graduate School of Engineering

## ARTICLE

# Precisely Controlled Molecular Imprinting of Glutathione-s-Transferase by Orientated Template Immobilization Using Specific Interaction with an Anchored Ligand on a Gold Substrate

Cite this: DOI: 10.1039/x0xx00000x

Received 00th January 2012,  
Accepted 00th January 2012

DOI: 10.1039/x0xx00000x

[www.rsc.org/](http://www.rsc.org/)

Yuri Kamon, Ryo Matsuura, Yukiya Kitayama, Tooru Ooya, and Toshifumi Takeuchi\*

We demonstrate a novel synthetic route for molecularly imprinted polymers (MIPs) thin films using a bottom-up approach utilizing protein/ligand specific interactions. The ligand was anchored on a gold substrate and served to (i) orient the immobilized target protein for precise formation of homogeneous binding cavities and (ii) act as a binding site with high affinity and selectivity on the MIP thin films after release of the immobilized protein. The MIP thin films were synthesized by controlled/living radical polymerization (CLRP), which allowed for precise control of the film thickness to optimize binding performance. A mixed self-assembled monolayer comprising anchored maleimide groups and bromoisobutryl groups was constructed on the gold substrate: the former oriented the immobilization of the target protein, and the latter initiated CLRP. The chosen model target protein and ligand were glutathione-s-transferase- $\pi$  (GST- $\pi$ ) and glutathione (GSH), a protein-specific ligand to GST- $\pi$ . The obtained MIP thin films of precisely controlled film thickness exhibited high affinity toward the target protein compared to non-imprinted polymer (NIP) thin films. Protein binding selectivity was investigated using a selectivity parameter ( $\alpha$ ) calculated by surface plasmon resonance response with reference proteins, human serum albumin (HSA) and fibrinogen (FIB). The results indicated that MIP film thickness affects protein binding selectivity: a polymer thickness of approximately 15 nm gave more selective protein binding (selectivity parameter for  $\alpha(\text{HSA}) = 0.09$  and for  $\alpha(\text{FIB}) = 0.30$ ). Furthermore, we clarified that a more hydrophilic polymer matrix in the presence of NaCl gave more selective binding of GST- $\pi$ . Our findings show that this bottom-up synthetic route has potential for facilitating the fabrication of highly specific MIPs as artificial protein recognition materials.

## Introduction

Molecular recognition materials for specific proteins have been attracting much attention in life science areas, including proteomics, biomaterials, and pathological diagnosis.<sup>1,2</sup> Bio-based materials such as antibodies and enzymes are commonly used as molecular recognition materials.<sup>3</sup> Although these bio-based materials have highly selective binding properties, these materials are difficult to produce and tend to be unstable and to denature. Therefore, polymer-based artificial molecular recognition materials that can be easily and inexpensively manufactured would be advantageous.

Molecular imprinting has exceptional potential for synthesizing artificial molecular recognition materials with specific binding cavities capable of recognizing target molecules.<sup>4-6</sup> Molecularly imprinted polymers (MIPs) have been typically prepared by copolymerization of functional monomer(s), a co-monomer, and a cross-linking agent in the presence of target molecules, which form a complex with the functional monomer(s). After removal of the

template, binding cavities complementary in size and shape are formed in the MIPs, where the target molecules can be bound with high selectivity and affinity. MIPs targeted for specific proteins have better chemical stability than natural antibodies and can be prepared inexpensively and easily. They are therefore good candidates for artificial protein-recognition materials in place of natural antibodies. The ability of MIPs to recognize specific target proteins was reported by several research groups.<sup>7-10</sup> However, random rotation of the target proteins unintentionally occurred during the molecular imprinting process, resulting in the formation of various shapes of binding cavities (i.e., heterogeneous binding cavities) at random positions in the MIPs. This resulted in low binding activity and selectivity of MIPs for the target protein.

To address this problem, molecular imprinting with immobilized template molecules on the substrate has recently been widely studied.<sup>11-23</sup> Immobilization of template molecules is an effective method to greatly reduce random rotation during the molecular imprinting process to provide specific binding cavities with high

affinity and selectivity toward the target protein.<sup>11</sup> We also previously reported that oriented template immobilization with crystallized protein dramatically improves the protein binding selectivity of MIP films compared to the use of non-crystallized protein.<sup>12</sup>

In order to prepare MIPs with high binding activity, it is also important to make use of functional monomers with high affinity and selectivity toward the target protein. These functional monomers act as binding sites on MIPs after the removal of the template protein. Generally, interactions between commonly used functional monomers and target proteins are weak, as they are primarily electrostatic and hydrophobic interactions; thus, they have a tendency to non-specifically interact with many amino acid residues, resulting in low protein binding selectivity by the MIP. On the other hand, protein/ligand specific interactions make it possible to induce high binding affinity and selectivity because the ligands interact only with site-specific amino acid residues inside the target protein with a high binding constant.<sup>24, 25</sup> In a previous report, Haupt et al. demonstrated the synthesis of MIP microgels as artificial enzyme inhibitors using a benzamidine-based functional monomer, where the benzamidine moiety acted as a protein-specific ligand for trypsin.<sup>26</sup>

In this paper, we demonstrate a novel synthetic route for producing MIP thin films that have high affinity and selectivity toward a target protein. The target protein is immobilized in a specific orientation on a gold substrate through protein/ligand specific interactions (Figure 1). The anchored ligand has two roles: 1) immobilizing the template protein on a gold substrate while greatly reducing the protein's potential for random rotation during polymerization, and 2) acting as a binding site after removal of the template protein, thereby allowing for high protein selectivity.

As a model target, we selected glutathione-s-transferase- $\pi$  (GST- $\pi$ ), a well-known cancer biomarker.<sup>27, 28</sup> GST- $\pi$  is commonly used in disease diagnosis as a biomarker because the levels of GST- $\pi$  in the serum of afflicted patients who have undergone surgery, as well as the levels in patients with either hemolytic anemia or leukemia anemia, are increased from the normal level. Moreover, GST- $\pi$  has a specific ligand, glutathione (GSH) which can interact with the G-site on GST- $\pi$ . This results in a specific protein/ligand interaction between GSH and GST- $\pi$  based on site-specific interactions between amino acid residues in the G-site (Ser A65, Arg A13, Asp B98, Gln A64, Leu A52, Trp A38) and amine, carboxyl and amide group moieties on the Glu, Cys and Gly residues in GSH. The binding affinity of GSH to GST- $\pi$  is  $5.5 \times 10^3 \sim 1.0 \times 10^4 \text{ M}^{-1}$ .<sup>29-31</sup>

label-free measurements and detects binding behavior with high sensitivity and accuracy. For oriented immobilization of GST- $\pi$  on a gold surface via GST- $\pi$ /GSH specific interactions, a mixed self-assembled monolayer (mixed SAM) comprising anchored maleimide groups and bromoisobutyryl groups was used as a platform (Figure 1). The maleimide group enables the SH in GSH to bind onto the mixed SAM. The bromo group works as an initiator for the surface-initiated activator generated by electron transfer for atom transfer radical polymerization (SI-AGET ATRP). This leads to precise control of the film thickness, where the cross-linked polymer matrix can be propagated proportionally to the polymerization time from the mixed SAM layer on the gold substrate.<sup>32-35</sup> Finally, we investigated the influence of binding conditions (*i.e.*, the balance between hydrophilicity and electrostatic forces within the MIPs) on protein binding selectivity.

Figure 2 (a) and (b) show the X-ray photoelectron spectra of S 2p and Br 3d, respectively, of the gold substrate before and after immersion in an ethanol solution of bis[2-(2-bromoisobutyryloxy)-undecyl] disulfide and (11-mercaptopundec-11-yl)tetra(ethyleneglycol), which were components of the mixed SAM. In Figure 2 (a), the S 2p peak, which was not observed before the treatment, appeared clearly after immersion of the gold substrate. The peak apex was observed at around 162 eV, indicating that the S group had chemically bound to the gold substrate, whereas if the molecules had bound physically, the apex would have appeared at around 164 eV.<sup>36</sup> Moreover, in Figure 2 (b), the Br 3d peak was observed more clearly after the immersion treatment than before.

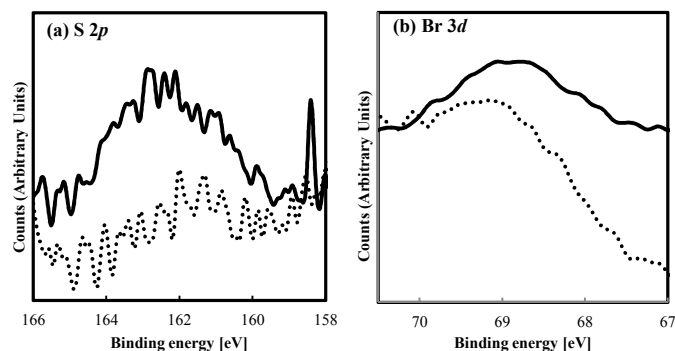


Figure 2. X-ray photoelectron spectra of S 2p (a) and Br 3d (b). solid line: after formation of mixed SAM; dotted line: before formation of mixed SAM.

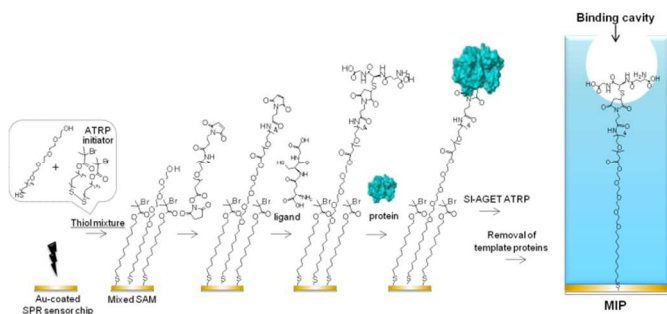


Figure 1. Preparation of MIP thin films for GST- $\pi$ .

## Results and Discussion

The binding activity of the MIP thin films on a gold substrate was evaluated by surface plasmon resonance (SPR). SPR allows for

The thickness of the mixed SAM on the gold substrate was measured by X-ray reflectometry (XRR) to be approximately 2.1 nm (Figure S1(a) in ESI). This value is in accordance with the theoretical thickness of the 2-(2-bromoisobutyryloxy)-undecyl group (ca. 2.0 nm), which should be highly ordered in a mixed SAM. These results indicate that the designed mixed SAM was successfully formed on the gold substrate.

Using the hydroxyl groups of the mixed SAM on the gold substrate, maleimide groups were attached via a condensation reaction with MAL-dPEG<sub>4</sub>-NHS in dry CH<sub>2</sub>Cl<sub>2</sub>.<sup>37</sup> Subsequently, the SH group on GSH reacted with the maleimide groups on the mixed SAM via Michael addition reaction, thereby anchoring the GSH onto the bromoisobutyrylated gold substrate. GST- $\pi$  was then immobilized on the anchored GSH via protein/ligand specific interactions.<sup>38</sup> It was very important to immobilize an oriented GST- $\pi$  onto the anchored GSH to obtain highly selective MIPs using the immobilized template on the gold substrate. To confirm that GST- $\pi$

was immobilized onto the gold substrate, we performed real-time monitoring of GST- $\pi$  immobilization by SPR measurements. The amount of GST- $\pi$  bound via conjugation with GSH immobilized on a gold substrate increased as the GST- $\pi$  concentration increased; the binding constant was calculated to be  $6.3 \times 10^3 \text{ M}^{-1}$  (Figure S2 in ESI). This value was comparable to that of free GSH and GST- $\pi$ .<sup>29</sup> The Scatchard plot indicated that the maximum amount of immobilized GST- $\pi$  was approximately  $10 \text{ fmol/mm}^2$ , which is approximately one sixth of the theoretical maximum binding capacity of GST- $\pi$  ( $66 \text{ fmol/mm}^2$ ), assuming that GST- $\pi$  is spherical with a diameter of ca. 5 nm. These results suggested that anchored GSH is an effective immobilizing ligand for GST- $\pi$  on a gold substrate, and that GST- $\pi$  was successfully immobilized to the anchored GSH on that gold substrate.

In the proposed molecular imprinting method, SI-AGET ATRP was carried out on the bromoisobutyrylated gold substrate bearing the immobilized GST- $\pi$ , using  $\text{Me}_6\text{TREN}$  as a copper ligand since it was reported to be an effective ligand for ATRP of acrylamide monomers.<sup>39-41</sup> After the polymerization, peaks at 3420 and 3450  $\text{cm}^{-1}$  derived from NH groups of acrylamide units appeared, which were not observed before the polymerization (Figure S3 in ESI). Compared with the results of XPS measurements for GSH-immobilized SAM and MIP thin films on gold substrates, new energy bands appeared only in the C1s spectrum of the MIP thin film, which could be derived from C=O and C-O bonds (Figure S4 in ESI), indicating that HEMA was copolymerized in the MIP thin film. Moreover, the Br groups remained on the film surface even after the polymerization. Controlling the polymer film thickness was critically important for the formation of appropriate binding cavities with high binding activity. If the polymerization time was too long, the polymer film was too thick to allow the template protein to be washed from the polymer film in order to form binding cavities after SI-AGET ATRP. The polymer film thickness measured by XRR increased linearly with increasing polymerization time, reaching just over 40 nm after 3 h (Figure 3 and Figure S1 (b-d) in ESI). These results indicate that SI-AGET ATRP could proceed from the bromo groups on the gold substrate, and that polymer film thickness could be controlled by changing the polymerization time. The estimated height of the GST- $\pi$  immobilized substrate was approximately 12 nm, since the thickness of mixed SAM was approximately 2 nm, the chain length of the linker for GST- $\pi$  immobilization was theoretically 4-5 nm, and the diameter of GST- $\pi$  was ca. 5 nm. Therefore, a MIP film thickness of approximately 12 nm should provide the required binding cavities on the surface substrate. Since the polymer thickness after 3 h of SI-AGET ATRP could be too large, burying GST- $\pi$  inside the polymer film, we selected a polymerization time of 1 h for the following experiments.

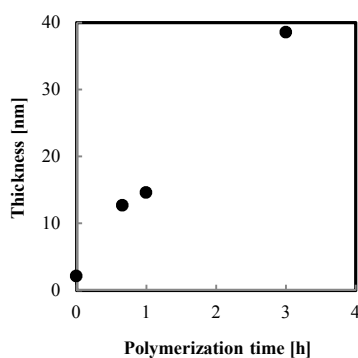


Figure 3. Time course of the film thickness formed on the GST- $\pi$ -immobilized gold substrate by SI-AGET ATRP.

The removal of the template protein GST- $\pi$  after the polymerization was confirmed by the SPR equipment. The template protein was washed with NaCl and SDS until the RU value became constant. After the removal of GST- $\pi$ , the binding cavities toward GST- $\pi$  were left in the MIP thin film since the MIP thin film was cross-linked, so that the polymer matrix was stable and could keep its conformation after the removal of GST- $\pi$ .

SPR measurements were performed to evaluate the binding activity of the prepared MIP thin films toward GST- $\pi$ . Since selection of a running buffer is important for GST- $\pi$  binding towards MIPs, we investigated the amount of GST- $\pi$  bound onto the MIP thin films in three running buffers: 10 mM Tris-HCl pH 7.4, 10 mM HEPES buffer pH 7.4, and 10 mM phosphate buffer pH 7.4. The binding isotherms and Scatchard plots (Figure S5 in ESI) suggested that the amount bound and the binding constant of GST- $\pi$  toward the MIP was largest in 10 mM Tris-HCl pH 7.4. Therefore, 10 mM Tris-HCl pH 7.4 was selected as the running buffer. The amount of GST- $\pi$  bound onto the MIP thin films increased with increasing protein concentrations: the  $\Delta\text{RU}/M_w$  value was approximately  $4.3 \text{ fmol/mm}^2$  when  $1 \mu\text{M}$  GST- $\pi$  was injected (Figure 4). A  $K_a$  value of  $6.4 \times 10^6 \text{ M}^{-1}$  was calculated by Scatchard analysis (Figure S6 in ESI). The plot was observed to be linear, indicating that 1:1 binding occurred between GST- $\pi$  and the binding cavity in the MIP thin films. The maximum amount of binding cavities in the film was calculated to be  $4.7 \text{ fmol/mm}^2$ , which is about half the amount of immobilized GST- $\pi$  before polymerization ( $10 \text{ fmol/mm}^2$ ).

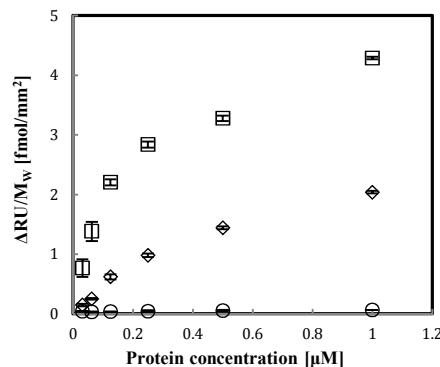


Figure 4. Binding isotherms of GST- $\pi$  towards MIP (square), NIP-GSH (diamond) and NIP-noGSH (circle) prepared with HEMA as a co-monomer in 10 mM Tris-HCl buffer pH 7.4 ( $n=3$ ).

Two non-imprinted polymer (NIP) thin films were prepared as controls. NIP-GSH was prepared by SI-AGET ATRP with immobilization of GSH but without immobilization of GST- $\pi$ , and NIP-noGSH was prepared without the immobilization of GSH. The binding activities of NIP-GSH and NIP-noGSH toward GST- $\pi$  were evaluated with SPR measurements. The amount of bound GST- $\pi$  ( $\Delta\text{RU}/M_w$  value) toward NIP-noGSH was essentially 0 at all GST- $\pi$  concentrations. In contrast, the  $\Delta\text{RU}/M_w$  value of bound GST- $\pi$  toward NIP-GSH increased gradually with increasing concentration of GST- $\pi$ , reaching approximately  $2.0 \text{ fmol/mm}^2$  at  $1 \mu\text{M}$  GST- $\pi$ . These results clearly indicated that a) GSH worked as an effective binding site on the MIP and NIP-GSH films, and b) the non-specific binding of GST- $\pi$  on the polymer matrix could be considered negligible because NIP-noGSH had essentially no binding affinity toward GST- $\pi$ . The  $K_a$  value of NIP-GSH was calculated from a Scatchard plot to be  $1.4 \times 10^6 \text{ M}^{-1}$  (Figure S6 in ESI), which is four times smaller than the  $K_a$  value of MIP. The maximum amount of

binding cavities in MIP ( $4.7 \text{ fmol/mm}^2$ ) was also slightly larger than the maximum amount of GST- $\pi$  bound toward NIP-GSH ( $3.7 \text{ fmol/mm}^2$ ). The amount of anchored GSH was almost the same between MIP and NIP-GSH before imprinting, but after the imprinting process, MIP produced binding cavities at the GSH anchored positions whereas NIP-GSH did not, because part of each anchored GSH was buried in the polymer matrix during SI-AGET ATRP. Therefore, the amount of GST- $\pi$  that could bind to NIP-GSH was smaller than with MIP. These results confirmed that binding cavities were successfully formed in the thin film by imprinting using the proposed synthetic route for MIP films.

Protein binding selectivity is an important functional parameter in MIPs. In this work, human serum albumin (HSA) and fibrinogen (FIB), which coexist with GST- $\pi$  in serum or plasma, were selected as reference proteins. In order to evaluate the protein binding selectivity of the MIPs, SPR measurements using GST- $\pi$ , HSA and FIB were performed. Then, the selectivity parameter ( $\alpha$ ) was calculated as an index of the selectivity, which was defined as the ratio of a  $\Delta\text{RU}/M_w$  value of  $0.5 \mu\text{M}$  HSA or FIB to that of  $0.5 \mu\text{M}$  GST- $\pi$  ( $M_w$ : molecular weight). The  $\Delta\text{RU}/M_w$  values of HSA and FIB were approximately  $0.3 \text{ fmol/mm}^2$  and  $1.9 \text{ fmol/mm}^2$ , both of which are smaller than that of GST- $\pi$  ( $3.3 \text{ fmol/mm}^2$ ), and the  $\alpha$  values were calculated to be 0.11 for HSA and 0.59 for FIB. As the results indicate, a MIP thin film with binding selectivity toward GST- $\pi$  was obtained using the present technique.

Minimizing non-specific binding of reference proteins (especially FIB) to MIPs is very important for obtaining MIPs with higher selective binding toward GST- $\pi$ . The interaction between the polymer surface and the protein occurs at the positively and/or negatively charged regions, as well as at the neutral, hydrophilic and hydrophobic regions.<sup>42</sup> At pH 7.4, the carboxyl groups (Glu and Gly) and the amino group (Glu) in GSH are, respectively, negatively and positively-charged; therefore, GSH has an overall negative charge at pH 7.4. Gok et al. reported more non-specific adsorption of FIB toward a poly(HEMA-co-acrylic acid) membrane containing a negative charge than to a nonionic poly(HEMA) at pH 7.4.<sup>42</sup> Their work clearly indicated that the negative charge on the polymer increased the non-specific binding of FIB toward that polymer. Therefore, it should be possible to minimize non-specific binding of reference proteins to MIPs by regulating the electrostatic interactions.

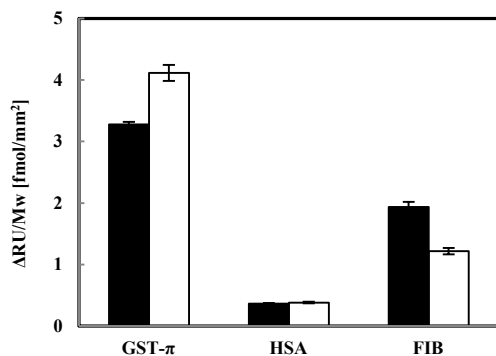


Figure 5. Effect of salt concentrations on the protein binding selectivity of MIP prepared with HEMA as a co-monomer in 10 mM Tris-HCl buffer pH 7.4 with (white) or without 140 mM NaCl (black) ( $n=3$ ).

We examined the effect of salt concentration in the running buffer used for SPR measurements on the protein binding selectivity of MIP in the presence or absence of NaCl (140 mM). NaCl was

maintained to approximately physiological concentrations. Using a running buffer with 140 mM NaCl, the amount of FIB bound to the MIP thin film decreased to  $1.3 \text{ fmol/mm}^2$  (a decrease of about 40%), likely due to the NaCl decreasing the electrostatic interactions between FIB and MIP (Figure 5). In addition, the amount of bound HSA remained low when the running buffer contained 140 mM NaCl. Interestingly, however, the amount of GST- $\pi$  bound to the MIP thin film increased by about 30% under these conditions. The  $\alpha$  values for HSA and FIB decreased to 0.09 and 0.30, respectively. In theory, if the target proteins bound to MIP thin films through only electrostatic interactions, the amount of bound protein should have decreased in the presence of 140 mM NaCl. However, Figure 5 shows that the amount of bound GST- $\pi$  increased, suggesting that the GST- $\pi$ /GSH specific interactions arise not only from electrostatic interactions, but also from van der Waals forces and hydrophobic interactions. Therefore, the salt in the running buffer depressed only the non-specific binding of reference proteins to the MIP thin films. Consequently, SPR binding experiments on the MIP thin films containing ligand-based binding sites should be carried out using running buffer containing 140 mM NaCl in order to decrease non-specific binding of reference proteins.

The effect of MIP film thickness on protein binding selectivity was examined (Figure 6). Before SI-AGET ATRP (GSH-immobilized substrate), strong non-specific binding of FIB was observed, even though the specific ligand, GSH, was present on the surface ( $\alpha_{\text{HSA}}$ , 0.46 and  $\alpha_{\text{FIB}}$ , 0.68). In contrast, after 1 h of SI-AGET ATRP, non-specific binding of both FIB and HSA decreased remarkably and the amount of bound GST- $\pi$  increased ( $\alpha_{\text{HSA}}$ , 0.09 and  $\alpha_{\text{FIB}}$ , 0.30). However, after 3 h, the affinity and selectivity were reduced ( $\alpha_{\text{HSA}}$ : 0.22 and  $\alpha_{\text{FIB}}$ : 0.37), suggesting that a too thick polymer film may bury GST- $\pi$  immobilized by the anchored GSH, decreasing the amount of binding cavities and/or the active GSH molecules on the surface.

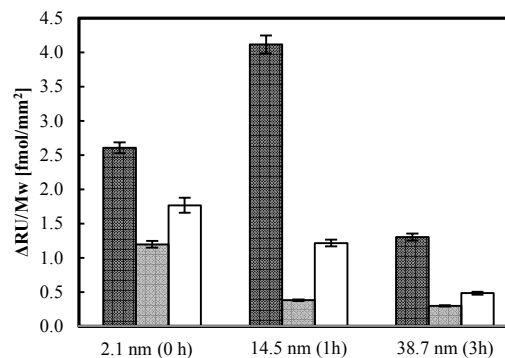


Figure 6. Effect of the MIP film thickness on the selectivity towards GST- $\pi$  (black), HSA (gray) and FIB (white) in 10 mM Tris-HCl buffer pH 7.4 containing 140 mM NaCl ( $n=3$ ). Protein concentration:  $0.5 \mu\text{M}$

We also investigated GST- $\pi$  binding kinetics toward GSH-immobilized substrate, MIP 1 h and MIP 3 h, using BIAevaluation software. Association rate constant  $k_a$  values were calculated to be  $1.62 \times 10^5 \text{ M}^{-1}\text{s}^{-1}$  for GSH-immobilized substrate,  $7.51 \times 10^4 \text{ M}^{-1}\text{s}^{-1}$  for MIP prepared by 1 h-SI-ATRP (MIP-1h), and  $3.35 \times 10^4 \text{ M}^{-1}\text{s}^{-1}$  for MIP prepared by 3 h-SI-ATRP (MIP-3h). The  $K_d$  values were estimated from a Scatchard plot to be  $1.32 \times 10^7 \text{ M}^{-1}$  for the immobilized-GSH (before polymerization, 0 h),  $2.55 \times 10^6 \text{ M}^{-1}$  for MIP-1h, and  $3.37 \times 10^6 \text{ M}^{-1}$  for MIP-3h (Figure S7 in ESI). These results indicated that the  $k_a$  and  $K_d$  values of GST- $\pi$  for GSH-

immobilized substrate are larger than those for MIPs, perhaps due to the high accessibility of GST- $\pi$  to the immobilized-GSH in the absence of the polymer layer. Alternatively, it could be due to differences between the binding mechanism of GST- $\pi$  to the immobilized-GSH and MIP thin films. The Scatchard plots for MIP thin films maintained linearity for all protein concentrations tested, indicating that the GST- $\pi$  binding mechanism towards MIP thin films is likely simple 1:1 binding, since the polymer layers prevent cross-talk between the binding cavities. On the other hand, the Scatchard plots for GSH-immobilized substrate could be separated into two linear plots, indicating the existence of two binding mechanisms. GST- $\pi$  has two G-sites capable of GSH binding on the plane-symmetrical position (Protein Data Bank ID: 7gss). Therefore, GST- $\pi$  binding behavior toward GSH-immobilized substrate presumably does not follow a simple 1:1 binding mechanism but rather a multi-point binding mechanism. It is likely that one anchored GSH first binds to a G-site followed by other GSH molecules binding to other G-sites, providing an apparently large association constant compared to that for MIP thin films.

In contrast, the protein binding selectivity of the immobilized-GSH was lower than that of the MIPs. These results indicate that a polymer layer of appropriate thickness is crucial for high affinity and selectivity; consequently, controlling polymer thickness is critical for precise molecular imprinting. Our approach used mixed SAM comprising bromo groups (initiator for SI-ATRP) and GST- $\pi$  attached via oriented immobilized GSH. This could provide more precise control of film thickness compared to previously reported approaches<sup>43</sup> because earlier techniques applied SI-ATRP to randomly positioned polymer chain end bromo groups on the core particles. In addition, in these earlier approaches, the immobilizing template was not always oriented because the orientation of the immobilized ligand was most likely disordered at the surface of the core particle.

Finally, we tried to decrease non-specific binding of the reference proteins by increasing the hydrophilicity of MIP thin films, since several groups have been reported that highly hydrophilic polymer films have low non-specific binding properties.<sup>44, 45</sup> *N*-[Tris(hydroxymethyl)methyl]acrylamide (THMA) was selected as the co-monomer instead of HEMA, as THMA is more hydrophilic than HEMA; the log *P* value of HEMA is 0.54 and of THMA is -2.19, as estimated by PALLAS 3.0 (CompuDrug Chemistry Ltd.). The water contact angle was also lower in MIP thin film prepared with THMA than that prepared with HEMA, indicating that use of THMA as a comonomer resulted in the higher hydrophilic MIP thin film. (Figure S8 in ESI) When MIP and NIP-GSH were prepared with THMA, the binding constant of MIP was larger than that of NIP-GSH (Figure S9 in ESI), indicating that binding cavities were formed in the MIP prepared with THMA, similar to HEMA-based MIP thin film. The binding behavior of MIP prepared with THMA was examined using the three proteins. Although the amount of GST- $\pi$  bound was approximately halved by changing the comonomer from HEMA to THMA, the selectivity was improved; in particular,  $\alpha_{\text{FIB}}$  decreased from 0.30 to 0.17 (Figure S10 in ESI). These results suggested that non-specific binding of FIB was prevented by using a more hydrophilic co-monomer, and the binding selectivity was improved.

## Conclusions

We have demonstrated the strategy of bottom-up fabrication of MIP thin films with oriented immobilized target protein using protein/ligand specific interactions between the target protein (GST- $\pi$ ) and the anchored ligand (GSH) on a gold substrate. GSH fulfilled two important roles: (i) it oriented GST- $\pi$  during the imprinting process, and (ii) it allowed for the creation of binding sites in the

imprinted cavities toward GST- $\pi$  after the removal of the template GST- $\pi$ . The obtained MIP thin films had high affinity and selectivity toward the target protein compared with NIP thin films, confirming that the imprinting effect was clearly derived from the proposed strategy. In addition, MIP thin films showed specific recognition for the target protein, showing that controlled film thickness is an important factor for binding selectivity. SI-AGET ATRP facilitated control of the MIP film thickness, resulting in the formation of imprinted cavities appropriate in size for the target protein and providing improved protein binding selectivity. We also clarified that non-specific binding of the reference proteins could be depressed by the addition of NaCl to the buffer solution without compromising specific binding toward GST- $\pi$ . Moreover, non-specific binding could be depressed by increasing the hydrophilicity of the MIP thin films using a more hydrophilic co-monomer, resulting in enhanced selectivity. From these results, our novel molecular imprinting synthetic route utilizing an anchored specific ligand shows promise as an effective method for synthesizing protein-imprinted thin films with high affinity and selectivity toward a target protein. This approach can now be readily applied to various pairs of biologically important protein-ligand specific interactions.

## Experiments

### Materials

Ethanol, CuBr<sub>2</sub>, L-ascorbic acid, 2-hydroxyethyl methacrylate (HEMA), ethylene diamine tetraacetic acid tetrasodium (EDTA-4Na) and human serum albumin (HSA) were purchased from Nacalai Tesque (Kyoto, Japan). Acrylamide, *N,N'*-methylenebisacrylamide (MBAA), and dichloromethane (Super Dehydrated or Wako 1st Grade) were purchased from Wako Pure Chemical Industries (Osaka, Japan). Wako 1st Grade dichloromethane was distilled before use. *N*-[Tris(hydroxymethyl)methyl]acrylamide (THMA), bis[2-(2-bromoisobutyryloxy)-undecyl] disulfide, (11-mercaptoundec-11-yl)tetra(ethyleneglycol), glutathione-*s*-transferase- $\pi$  (GST- $\pi$ ), tris(dimethylamino)ethylamine (Me<sub>6</sub>TREN) and L-glutathione (reduced form) (GSH) were purchased from Sigma-Aldrich (USA). Fibrinogen from human plasma was purchased from Calbiochem. *N*-hydroxysuccinimidyl-15-(3-maleimidopropionyl)-amido-4,7,10,13-tetraoxapentadecanoate (MAL-dPEG<sub>4</sub>-NHS ester) was purchased from Toyobo Co., Ltd. (Osaka, Japan). All water used was obtained from a Millipore Milli-Q purification system. Au-coated SPR sensor chips (superficial area: 120 mm<sup>2</sup>) were purchased from GE Healthcare (Tokyo, Japan). Au substrates for X-ray photoelectron spectroscopy (XPS) and X-ray reflectometry (XRR) measurement were purchased from JASCO Corporation (Tokyo, Japan).

### Apparatus

X-ray photoelectron spectra were obtained using XPS (JPS-9010MC, JEOL Ltd., Tokyo, Japan and PHI X-tool, ULVAC-PHI Inc., Kanagawa, Japan). Polymeric films thicknesses were measured using XRR (SmartLab 3kW, Tokyo, Japan). Surface Plasmon resonance (SPR) measurements were performed on a Biacore 3000 (GE Healthcare Japan, Tokyo, Japan).

### Preparation of the mixed self-assembled monolayer (mixed SAM)

Typical procedure is as follows. Au-coated SPR sensor chips were rinsed with ethanol and distilled water, then cleaned by UV-O<sub>3</sub> treatment (20 min) or Ar etching (5 mA, 10 sec). The cleaned substrates were immersed in an ethanolic solution of 0.5 mM bis[2-

(2-bromoisobutyryloxy)-undecyl] disulfide and 0.5 mM (11-mercaptopundec-11-yl)tetra(ethyleneglycol) for 24h at 25°C. Afterwards, the mixed SAM-formed SPR sensor chips were thoroughly washed with ethanol and distilled water, dried in a stream of nitrogen, and stored under vacuum pressure.

#### Maleimidation of the mixed SAM

The mixed SAM-formed SPR sensor chips were immersed in a dried CH<sub>2</sub>Cl<sub>2</sub> solution containing 5 mM MAL-dPEG<sub>4</sub>-NHS ester overnight at 25°C for maleimidation on the surface of the mixed SAM. After maleimidation, the chips were washed with dried CH<sub>2</sub>Cl<sub>2</sub>, ethanol, and distilled water and dried in a stream of nitrogen.

#### Immobilization of L-glutathione (GSH) on the maleimidated mixed SAM

The maleimidated SPR sensor chips were incubated for 2 h in 15 mM PBS buffer (pH 7.4) containing GSH (1 mg/mL, reduced form) at 25°C to yield GSH-attached mixed SAM surfaces. The chips were rinsed with distilled water and dried in a stream of nitrogen.

#### Immobilization of GST- $\pi$

The GSH-attached SPR sensor chips were submerged in a 100  $\mu$ g/mL GST- $\pi$  solution in a 15mM PBS buffer (pH 7.4) for 1h at 25°C to immobilize GST- $\pi$  by protein/ligand interactions. The chips were then rinsed with distilled water and dried in a stream of nitrogen.

#### Preparation of MIPs by SI-AGET ATRP

Typical procedure of preparation of MIPs by SI-AGET ATRP is as follows. Co-monomers acrylamide (4.5 mM) and HEMA (445.5 mM), which play the role of controlling the degree of cross-linkage and hydrophilicity of the polymer film, MBAA (50 mM), CuBr<sub>2</sub> (10 mM), and Me<sub>6</sub>TREN (10 mM) were dissolved in 10 mM HEPES buffer (pH 7.4). GST- $\pi$  immobilized SPR sensor chips were fixed in a Teflon cell and submerged in this pre-polymer solution so that only one surface of the sensor chip was exposed to the solution. They were then thoroughly purged by vacuum pressure then flushed with nitrogen gas. A degassed 10 mM HEPES buffer (pH 7.4) containing ascorbic acid (10 mM) was added via syringe to this solution. The solution was degassed, and polymerization was induced in a water bath at 40°C for 1h. For the THMA-based polymer, 15 mM PBS buffer (pH 7.4) was used as a solvent and SI-AGET ATRP was carried out for 3h at 30°C. After polymerization, the chips were washed with pure water and submerged in 1M EDTA-4Na aqueous solution for 4h to remove the Cu(II) ions remaining in the polymeric thin films, and then the chips were washed with pure water and dried in a stream of nitrogen. The template protein was removed using 1M NaCl, 0.5 w% SDS or 0.5 w% SDS containing 150 mM NaCl using the SPR equipment until the RU value became constant.

#### Preparation of non-imprinted polymers (NIPs); NIP-GSH and NIP-noGSH by SI-AGET ATRP

NIP-GSH was obtained using the same conditions as SI-AGET ATRP preparation, but without the immobilization of GST- $\pi$ . NIP-noGSH was also obtained using the same conditions as SI-AGET ATRP preparation, but without the immobilization of GSH and GST- $\pi$ .

#### XPS measurements

The formation of the mixed SAM on a gold substrate (glass-Cr (40 nm)-Au (50 nm)) was evaluated by XPS (JPS-9010MC). The

conditions of the XPS measurements were as follows: source: Mg K $\alpha$  (10 kV, 20 mA); takeoff angle: 60°; initial survey scans: 0-1000 eV binding energy. Compositional survey and detail scans for S2p and Br 3d were acquired using a detector pass energy of 30 eV centered at the binding energies of 162 and 69 eV, respectively. GSH-immobilized substrates and MIP thin films were evaluated by XPS (PHI X-tool). The conditions of the XPS measurements were as follows: source: Al K $\alpha$  (20 kV, 101 W); takeoff angle: 45°. Compositional survey scans were carried out 0-1000 eV binding energy using a detector pass energy of 69 eV. Narrow scans for O 1s, C 1s, N 1s, S 2p, and Br 3d were acquired using a detector pass energy of 112 eV.

#### XRR measurements

The thicknesses of the MIP polymer thin films consisting of acrylamide, HEMA and MBAA prepared by SI-AGET ATRP were measured by XRR. The conditions of XRR were as follows: source: CuK $\alpha$  radiation,  $\lambda=0.154$  nm; measured area: 1.0 $\times$ 1.0 cm; angle range (2 $\theta$ ): 0.0-6.0°. Obtained oscillation patterns of X-ray reflective profiles were analyzed by X-ray reflectivity analysis software GXRR with Parratt theory, and the parameters (thickness, density, and interfacial roughness) of thin films were determined.<sup>46</sup>

#### SPR measurements

GST- $\pi$ , HSA and Fib (0-1.0  $\mu$ M), each dissolved in 10 mM Tris-HCl buffer (pH 7.4) with and without 140 mM NaCl, were used for these experiments. Flow rate was 20  $\mu$ L/min and injection volume was 20  $\mu$ L. Regeneration solutions were selected appropriately from the following candidates: 1M NaCl<sub>aq</sub>, 0.5 w% SDS<sub>aq</sub>, 0.3 w% SDS<sub>aq</sub>, 0.5 w% SDS + 150 mM NaCl<sub>aq</sub>, and 0.075 w% SDS + 150 mM NaCl<sub>aq</sub>. The optimal regeneration solutions were injected once or twice for 30 sec or 60 sec until protein RU intensity signals reached a steady RU value. The amount of bound protein was calculated from the signal intensity (resonance units, RU; 1 RU corresponds to about 1 pg/mm<sup>2</sup> of bound protein<sup>47</sup> at 150 sec after protein injection). All binding experiments were repeated three times. Binding isotherms were drawn using  $\Delta$ RU values for each protein concentration.

SPR sensorgrams of GST- $\pi$  toward GSH-immobilized substrate and MIPs were kinetically analyzed by using BIAevaluation software with fitting formula as follows.

$$\text{Dissociation area: } RU = RU_0 \times \exp \{-k_d (t-t_0)\} + \text{Offset}$$

$$\text{Association area: } RU = \{k_a C R_{\text{max}} / (k_a C + k_d)\} \times \{1 - \exp (-k_a C + k_d) (t-t_0)\} + \text{RI}$$

RU is resonance units of each instant of time t, RU<sub>0</sub> is the RU value at the commencement of dissociation starting, k<sub>d</sub> is dissociation ratio constant, t<sub>0</sub> is the dissociation starting time in the dissociation area and the association starting time in the association area, Offset and RI are bulk effect RU values, k<sub>a</sub> is the association ratio constant, C is the injected protein concentration, R<sub>max</sub> is the theoretical maximum response.

#### Notes and references

Graduate School of Engineering, Kobe University  
1-1 Rokkodai-cho, Nada-ku, Kobe 657-8501, Japan  
Electronic Supplementary Information (ESI) available: [Detailed XRR data; Binding behaviour of GST- $\pi$  towards various substrates]. See DOI: 10.1039/b000000x/

1. R. E. Babine and S. L. Bender, *Chem. Rev.*, 1997, **97**, 1359-1472.
2. J. M. Lehn, *Angew. Chem. Int. Ed. in Eng.*, 1990, **29**, 1304-1319.
3. D. Lane and H. Koprowski, *Nature*, 1982, **296**, 200-202.

4. G. Wulff, *Angew. Chem. Int. Ed. in Eng.*, 1995, **34**, 1812-1832.
5. K. Mosbach, *Trends Biochem. Sci.*, 1994, **19**, 9-14.
6. M. Tatemichi, M. A. Sakamoto, M. Mizuhata, S. Deki and T. Takeuchi, *J. Am. Chem. Soc.*, 2007, **129**, 10906-10910.
7. N. W. Turner, C. W. Jeans, K. R. Brain, C. J. Allender, V. Hlady and D. W. Britt, *Biotechnol. Prog.*, 2006, **22**, 1474-1489.
8. D. E. Hansen, *Biomaterials*, 2007, **28**, 4178-4191.
9. D. Cai, L. Ren, H. Z. Zhao, C. J. Xu, L. Zhang, Y. Yu, H. Z. Wang, Y. C. Lan, M. F. Roberts, J. H. Chuang, M. J. Naughton, Z. F. Ren and T. C. Chiles, *Nature Nanotech.*, 2010, **5**, 597-601.
10. T. Takeuchi and T. Hishiya, *Org. Biomol. Chem.*, 2008, **6**, 2459-2467.
11. L. J. Liu, J. J. Zheng, G. J. Fang and W. H. Xie, *Anal. Chim. Acta*, 2012, **726**, 85-92.
12. T. Matsunaga and T. Takeuchi, *Chem. Lett.*, 2006, **35**, 1030-1031.
13. F. Bonini, S. Piletsky, A. P. F. Turner, A. Speghini and A. Bossi, *Biosens. Bioelectron.*, 2007, **22**, 2322-2328.
14. P. C. Chou, J. Rick and T. C. Chou, *Anal. Chim. Acta*, 2005, **542**, 20-25.
15. H. Q. Shi, W. B. Tsai, M. D. Garrison, S. Ferrari and B. D. Ratner, *Nature*, 1999, **398**, 593-597.
16. K. El Kirat, M. Bartkowski and K. Haupt, *Biosens. Bioelectron.*, 2009, **24**, 2618-2624.
17. T. Shiomi, M. Matsui, F. Mizukami and K. Sakaguchi, *Biomaterials*, 2005, **26**, 5564-5571.
18. R. Z. Ouyang, J. P. Lei and H. X. Ju, *Chem. Commun.*, 2008, 5761-5763.
19. C. J. Tan, M. G. Chua, K. H. Ker and Y. W. Tong, *Anal. Chem.*, 2008, **80**, 683-692.
20. J. X. Liu, K. G. Yang, Q. L. Deng, Q. R. Li, L. H. Zhang, Z. Liang and Y. K. Zhang, *Chem. Commun.*, 2011, **47**, 3969-3971.
21. W. Lei, Z. H. Meng, W. B. Zhang, L. Y. Zhang, M. Xue and W. Wang, *Talanta*, 2012, **99**, 966-971.
22. O. Hayden, K. J. Mann, S. Krassnig and F. L. Dickert, *Angew. Chem. Int. Ed.*, 2006, **45**, 2626-2629.
23. S. E. Williams, *PhD dissertation*, Cardiff University, UK.
24. N. J. Lynch, P. K. Kilpatrick and R. G. Carbonell, *Biotechnol. Bioeng.*, 1996, **50**, 151-168.
25. G. M. Verkhivker and P. A. Rejto, *Proc. Natl. Acad. Sci. U. S. A.*, 1996, **93**, 60-64.
26. A. Cutivet, C. Schembri, J. Kovensky and K. Haupt, *J. Am. Chem. Soc.*, 2009, **131**, 14699-14702.
27. D. Burg, J. Riepsaame, C. Pont, G. Mulder and B. van de Water, *Biochem. Pharmacol.*, 2006, **71**, 268-277.
28. J. Noguti, L. F. Barbisan, A. Cesar, C. D. Seabra, R. B. Choueri and D. A. Ribeiro, *In Vivo*, 2012, **26**, 647-650.
29. A. M. Caccuri, G. Antonini, P. Ascenzi, M. Nicotra, M. Nuccetelli, A. P. Mazzetti, G. Federici, M. Lo Bello and G. Ricci, *J. Biol. Chem.*, 1999, **274**, 19276-19280.
30. A. J. Oakley, M. LoBello, A. Battistoni, G. Ricci, J. Rossjohn, H. O. Villar and M. W. Parker, *J. Mol. Biol.*, 1997, **274**, 84-100.
31. C. Dsilva, *Biochem. J.*, 1990, **271**, 161-165.
32. K. Matyjaszewski and J. H. Xia, *Chem. Rev.*, 2001, **101**, 2921-2990.
33. K. Min, H. F. Gao and K. Matyjaszewski, *J. Am. Chem. Soc.*, 2005, **127**, 3825-3830.
34. T. Morinaga, M. Ohkura, K. Ohno, Y. Tsujii and T. Fukuda, *Macromolecules*, 2007, **40**, 1159-1164.
35. Y. Tsujii, K. Ohno, S. Yamamoto, A. Goto and T. Fukuda, in *Surface-Initiated Polymerization I*, ed. R. Jordan, 2006, vol. 197, pp. 1-45.
36. K. E. Nelson, L. Gamble, L. S. Jung, M. S. Boeckl, E. Naemi, S. L. Golledge, T. Sasaki, D. G. Castner, C. T. Campbell and P. S. Stayton, *Langmuir*, 2001, **17**, 2807-2816.
37. B. Nagel, N. Gajovic-Eichelmann, F. W. Scheller and M. Katterle, *Langmuir*, 2010, **26**, 9088-9093.
38. K. Park, J. Ahn, S. Yeon, M. Kim and B. H. Chung, *Biochem. Biophys. Res. Commun.*, 2008, **368**, 684-689.
39. M. Teodorescu and K. Matyjaszewski, *Abstracts of Papers of the American Chemical Society*, 1999, **218**, U541-U541.
40. M. Teodorescu and K. Matyjaszewski, *Macromolecules*, 1999, **32**, 4826-4831.
41. M. Teodorescu and K. Matyjaszewski, *Macromol. Rapid Commun.*, 2000, **21**, 190-194.
42. E. Gok, M. Kiremitci and I. S. Ates, *Reactive Polymers*, 1994, **24**, 41-48.
43. H. Zhang, J. Jiang, H. Zhang, Y. Zhang and P. Sun, *ACS Macro Lett.*, 2013, **2**, 566-570.
44. D. A. Musale and S. S. Kulkarni, *J. Memb. Sci.*, 1996, **111**, 49-56.
45. J. F. Hester, P. Banerjee and A. M. Mayes, *Macromolecules*, 1999, **32**, 1643-1650.
46. L. G. Parrat, *Phys. Rev.*, 1954, **95**, 359-369.
47. E. Stenberg, B. Persson, H. Roos and C. Urbaniczky, *J. Colloid Interface Sci.*, 1991, **143**, 513-526.